Non-coding RNA Research 9 (2024) 221–235

Contents lists available at ScienceDirect

Non-coding RNA Research

journal homepage: www.keaipublishing.com/en/journals/non-coding-rna-research

Original Research Article

lncRNA CERS6-AS1 upregulates the expression of ANLN by sponging miR-424-5p to promote the progression and drug resistance of lung adenocarcinoma

Zhuo Ting [a,1], Zuotao Wu [b,1], Chuyi Yang [a,1], Zihao Li [b], Hongyu Huang [a], Jinyan Gan [a], Nijiao Li [a], Xiaohong Li [a], Jueqi Lyu [a], Yanbin Wu [a,**], Shouming Qin [a,*]

[a] Department of Pulmonary and Critical Care Medicine, The First Affiliated Hospital of Guangxi Medical University, Nanning 530021, China
[b] Department of Cardio-Thoracic Surgery, The First Affiliated Hospital of Guangxi Medical University, Nanning 530021, China

ARTICLE INFO

Keywords:
CERS6-AS1
miR-424-5p
ANLN
Lung adenocarcinoma

ABSTRACT

Long non-coding RNAs (lncRNAs) play a crucial role in tumor generation and progression. However, the exact functional significance and underlying molecular mechanism by which lncRNA CERS6-AS1 operates in the context of lung adenocarcinoma (LUAD) remain unknown. We aimed to evaluate the potential role of the CERS6-AS1/miR-424-5p/ANLN axis in the progression of LUAD through bioinformatics and cytobehavioral experiments, and to provide a new insight into the combined treatment of LUAD. Based on the TCGA database, the expression of CERS6-AS1 in pan-cancer was evaluated, and its prognostic performance in LUAD was evaluated by ROC curve, survival curve and COX analysis. In addition, quantification of CERS6-AS1 expression levels in LUAD patients and lung cancer cells using quantitative real-time polymerase chain reaction (RT-qPCR), and further validate the functional significance of CERS6-AS1 in promoting the proliferation, migration, and invasion abilities of lung cancer cells. The competitive endogenous RNA (ceRNA) network was constructed, and miR-424-5p inhibitors were applied to CERS6-AS1 knockdown cells. The potential downstream genes associated with the regulatory axis of CERS6-AS1/miR-424-5p were analyzed by PPI network and gene enrichment analysis (KEGG). Finally, we evaluated the prognostic value of high expression of ANLN in LUAD and its effects on immune cell infiltration, tumor mutation burden, chemotherapy response, and immunotherapy. CERS6-AS1 expression was significantly elevated in both LUAD patients and lung cancer cells. In the CERS6-AS1 knockdown assay, the proliferation, invasion, migration and epithelial-mesenchymal transformation (EMT) of cancer cells were significantly inhibited. Notably, there was a prominent upregulation of miR-424-5p expression in cells where CERS6-AS1 was knocked down. Co-transfection of siRNA and miR-424-5p inhibitors into lung cancer cells restored the restriction on lung cancer cells. Anillin (ANLN) has been identified as a potential target gene for miR-424-5p and as a prognostic and immune biomarker associated with immune cell infiltration and tumor mutational burden in LUAD. Additionally, ANLN impacts the efficacy of chemotherapy and immunotherapy in LUAD patients. This study reveals a novel regulatory mechanism in which CERS6-AS1 may contribute to the progression of LUAD by influencing the expression of ANLN as a competitive sponge for miR-424-5p.

1. Introduction

Lung cancer has become a pressing global public health issue, posing a substantial burden on socio-economic development. It accounts for about 11.6 % of all new cancer cases worldwide and is associated with alarming mortality rates, leading to nearly 10 million deaths annually. What is concerning is that both the incidence and mortality rates of lung cancer are on the rise [1]. Lung carcinoma can be categorized into two types: non-small cell lung cancer (NSCLC) and small cell lung cancer (SCLC), with NSCLC comprising 80 % of lung cancer cases. It is disheartening to note that the five-year overall survival rate for NSCLC is merely 15 % [2]. Lung adenocarcinoma (LUAD) is recognized as the

* Corresponding author.
** Corresponding author.
E-mail addresses: yanbin_w2021@126.com (Y. Wu), qinshouming2019@163.com (S. Qin).
[1] These authors contributed equally to this work.

https://doi.org/10.1016/j.ncrna.2023.11.013
Received 11 September 2023; Received in revised form 27 November 2023; Accepted 28 November 2023
Available online 1 December 2023

most frequent subtype of NSCLC in recent years. It is associated with a poor prognosis, low survival rates, and has witnessed a substantial increase in incidence in recent years [3]. Advancing the diagnosis and treatment of LUAD has become a prominent research focus. In addition to conventional radiotherapy and chemotherapy, there is ongoing progress in novel approaches for LUAD management. These include targeted therapies, immune cell reconstruction within the tumor microenvironment, and advancements in oncogene methylation. These emerging strategies contribute to the continuous development and improvement of the management of LUAD [4–6]. Despite the promising results in the treatment of LUAD, there is still a need for further exploration and advancement in therapeutic options. In this study, we discovered a previously unreported long non-coding RNA (lncRNA) known as CERS6 antisense RNA 1 (CERS6-AS1). We found that CERS6-AS1 plays a part in enhancing cell growth and lymphatic metastasis in LUAD by sponging microRNA-424-5p (miR-424-5p). Moreover, our findings successfully predict Anillin (ANLN) as the downstream regulatory gene of this regulatory axis.

LncRNAs are a diverse class of noncoding RNAs that make up more than 98 % of the human transcriptome. These molecules are longer than 200 nucleotides and do not code for protein. Nevertheless, they are highly involved in the regulation of gene transcription and can interact with RNA, DNA, and protein. The functions and mechanisms of action of lncRNAs are complex and still being explored, but they play a crucial role in various cellular processes and have significant implications for gene regulation [7]. Dysregulation of lncRNAs is a common occurrence in cancer, and their aberrant expression is thought to have a significant impact on the development of cancer. One of the mechanisms by which lncRNAs exert their influence is by competitively binding with microRNAs (miRNAs). Therefore, lncRNAs can sponge miRNAs and prevent them from binding to the target mRNAs, thereby affecting the transcription of downstream target genes. This dysregulation of target gene expression by lncRNAs contributes to the complex molecular landscape of cancer and can have profound effects on tumorigenesis and disease progression [8]. The lncRNA CERS6-AS1 has been found to exhibit oncogenic properties in breast cancer, hepatocellular carcinoma, and pancreatic cancer [9–11]. As a class of short noncoding RNA molecules about 20–25 nucleotides in length, miRNAs have a crucial regulatory role in target gene expression. Found in eukaryotes, these endogenous molecules exert their function by binding to the 3′ untranslated region (UTR), resulting in target gene degradation or silencing [12]. The miR-424-5p miRNA has been strongly associated with various diseases, including hepatocellular carcinoma, ovarian cancer, and NSCLC [13]. Moreover, the inflammatory factor lncRNA circSLCO3A1 has been found to induce inflammation and apoptosis in human alveolar epithelial cells, which is achieved by competitively sponging with miR-424-5p, thereby activating the HMGB3 axis [14]. ANLN encodes an actin-binding protein, which is mainly located in the cytoskeleton and nucleus, and plays a role in cell proliferation and migration as well as cytoplasmic division [15]. ANLN expression has been found to increase significantly in a variety of cancers, including lung cancer, gastric cancer, breast cancer, bladder urothelial carcinoma, etc., and is associated with promoting tumor progression and poor prognosis. In addition, ANLN leads to immune tolerance and drug resistance of tumor cells by promoting the infiltration of immunosuppressive lymphocytes [16–19].

In this study, our objective was to investigate the functional and molecular mechanism of CERS6-AS1 in LUAD progression. Our findings demonstrated that CERS6-AS1 exhibited significant overexpression in both LUAD tissues and cells. This overexpression was found to be associated with aggressive clinicopathological characteristics and poor prognosis. Through CERS6-AS1 silencing experiments, we observed the capacity of lung cancer cell to proliferate, invade, migrate, and epithelial-mesenchymal transition (EMT) were significantly inhibited. Further investigation revealed that CERS6-AS1 by sponging miR-424-5p, increased the expression of ANLN, resulting in increased oncogene amplifications and mutations, and improved immune tolerance and drug resistance of tumor cells. Overall, our results suggest that CERS6-AS1 has the potential to regard as both a diagnostic marker and therapeutic target for LUAD.

2. Materials & methods

2.1. Data mining

LncRNAs data were obtained from TCGA. The TIMER2.0 database shows the expression of CERS6-AS1 in pan-cancer [20]. The DESeq2 package was used to calculate lncRNAs differentially expressed genes (DEGs) in LUAD, and CERS6-AS1 was labeled in the volcano map [21]. CERS6-AS1 was evaluated as a diagnostic biomarker for LUAD by constructing ROC curve. GEPIA is used to achieve the Kaplan-Meier survival curve estimation (K-M curve) of CERS6-AS1 [22]. Additionally, univariate COX was used to evaluate the effects of CERS6-AS1 expression and various clinical features on the prognosis of LUAD patients, and all independent prognostic factors were included for multivariate COX analysis in order to evaluate the independent contribution of each factor to the progression of LUAD. Transcripts Per Million (TPM) data of CERS6-AS1 in 30 normal tissues and 401 LUAD tissues was obtained from TCGA to compare the relative expression of CERS6-AS1 in LUAD. Screening of possible miRNAs for CERS6-AS1 based on TargetScan, Starbase v2 and ENCORI databases [23–25]. Screen for possible mRNAs for CERS6-AS1/miR-424-5p based on TargetScan, miRDB, and RAID databases, and their associations were illustrated using Sankey plot [26, 27]. Node genes were screened from PPI networks and analyzed functional enrichment in DAVID, the results of which were plotted using a Sankey plot (https://www.bioinformatics.com.cn, last accessed July 15, 2023) [28,29].

2.2. Clinical samples

Thirty-five clinical samples were collected from the Department of Thoracic Surgery, First Affiliated Hospital of Guangxi Medical University. Patient information is presented in Table 1.

2.3. RNA extraction and RT-qPCR

According on the manufacturer's protocol, RNAiso Plus (Takara, Japan) is added to fresh tissue samples or cells and total RNA is extracted

Table 1
Association of relative CERS6-AS1 expression with clinical features of patients.

Variables	n	M (p25, p75)	Z	P
Gender			−0.842	0.4
Female	17	5.9073(0.8839,7.4015)		
Male	18	1.8025(1.0414,3.6305)		
Age(years)			−0.515	0.606
young	11	4.5948(1.0257,7.6741)		
old	24	2.0211(0.9355,5.9159)		
Tumor size(cm)			−1.061	0.289
≤3	30	2.6286(1.126,6.9435)		
> 3	5	1.057(0.5582,4.8848)		
History of smoking			−1.023	0.307
No	25	1.7013(0.7079,6.8211)		
Yes	10	3.0005(1.6492,5.4186)		
Differentiation			−0.852	0.394
Well	12	2.2252(0.6803,5.5664)		
Poor + Moderate	23	2.2397(1.057,7.3107)		
Lymph node metastasis			−1.739	0.082
No	32	0.9277(1.7921,6.1131)		
Yes	3	4.5948(6.8211, NA)		
TNM stage			−0.804	0.422
I	31	1.8025(1.0257,6.176)		
II + III	4	5.7079(1.348,8.3935)		

1. Wilcoxon's rank-sum test for comparison of the two groups.
2. NA, null-able values.

at 4 °C, followed by reverse transcription of 1.0 μg of RNA to cDNA using Prime Script RT Master Mix (Takara). Gene expression levels were measured using the SYBR Green PCR Kit (Servicebio, China) in the Roche LC480II real-time PCR instrument. The relative quantitative expression of CERS6-AS1 and GAPDH was analyzed using the 2−ΔΔCt method [30]. Table 2 shows the primers used in this study. (Sangon Biotechnology & Nanning Gensis Biotechnology Ltd, China)

2.4. Cell culture and RNA interference

BEAS-2B bronchial epithelial cells and A549 cell lines were purchased from the Chinese Academy of Sciences (China), H1975 and H1299 LUAD cells were supplied by Wuhan Procell Life Technology Co., Ltd (China). BEAS-2B and A549 cells were cultured in Dulbecco's modified Eagle's medium (DMEM, Gibco, USA), H1975 and H1299 cells were cultured in Roswell Park Memorial Institute-1640 medium (RPMI-1640, Gibco) containing 1 % penicillin/streptomycin P1400 (Solarbio, China) and 10 % fetal bovine serum (FBS, Gibco). All cell lines were maintained at 37 °C and 5 % CO2 in a sterile and pollution-free incubator and then exposed to Small interfering RNA (siRNA, Guangzhou Ribobio Co., Ltd, China) using Lipofectamine 8000 (Beyotime, China) in serum-free medium (Gibco) after the cultured cell lines enter the logarithmic growth phase. The si-CERS6-AS1 sequences used were 5′-CCACTTACCTAACACCTGA-3′, 5′-CGCTGCTGATAACCAGTTT-3′, and 5′-CTAACACCTGAGATCTTAT-3′, respectively. After successful transfection, qPCR was used to detect CERS6-AS1 knockdown efficiency, and the siRNA with the most significant knockdown efficiency was selected for subsequent experiments.

2.5. Dual-luciferase assay

To confirm the targeting relationship between lncRNA CERS6 and miR-424-5p, the miR-424-5p mimic, miR-424-5p NC and wild-type and mutant CERS6-AS1 were transfected into the lung cancer cell lines using Lipo8000. The plasmid sequences of wild type and mutant CERS6-AS1 were 5 ′-GUUUUGUACUUAACGACG-3′ and 5 ′-TAAAATAT-TTTGCTGC-3′, respectively (Guangzhou Ribobio Co., Ltd). Similarly, we also verified the targeting relationship between miR-424-5p and ANLN, and the plasmid sequences of wild type and mutant ANLN were 5 ′-TTAAAGCATGAG-GCTGT-3′ and 5′-ATCATGGAAGTG-TCAGA-3′, respectively (HanBio Technology, China). After 48 h of transfection, the cells were lysed with lysis buffer for 15 min at 4 °C. The supernatants were placed in a non-luminescent 96-well plate, luminescent solution was added separately, firefly and sea kidney fluorescence (Promega, USA) were measured, and the ratio between the two was calculated.

2.6. Cell Counting Kit-8

A549 and H1299 cells (1×10^4/mL) were seeded in 96-well plates, then si-CERS6-AS1 and si-NC were transfected into experimental group and control group, respectively. Cell Counting Kit-8 (Biosharp, China) is mixed with 10 % complete medium to form a 10 % CCK-8 mixture, and 100 μL/well of the mixture was added to the A549 and H1299 cells. These cells were incubated in a sterile incubator for 4 h before each absorbance measurement and measure the optical density (OD) at 0 h, 24 h, 48 h, and 72 h. Delete the highest and lowest values and average the remaining values to obtain the proliferation level.

Table 2
RT-qPCR primer sequences.

Primer	Sequence (5'–3')	
CERS6-AS1	Forward	GCAGCCCAGCAGAAGTAG
	Reverse	GAGCATAGGGAAGCAACTCTCAG
miR-195-5p		CGTAGCAGCACAGAAATATTGGC
miR-15a-5p		GCTAGCAGCACATAATGGTTTGTG
miR-15b-5p		GCTAGCAGCACATCATGGTTTACA
miR-424-5p		GCCAGCAGCAATTCATGTTTTGAA
miR-16-5p		GTAGCAGCACGTAAATATTGGCG
U6	Forward	CTCGCTTCGGCAGCACA
	Reverse	AACGCTTCACGAATTTGCGT
ANLN	Forward	ACTCCAAAGCGACTCCTCAC
	Reverse	TCGCACAGCACTAAGACCTC
β-acting	Reverse	AGATCAAGATCATTGCTCCTCCTG
	Reverse	AGTCATAGTCCGCCTAGAAGCAT

2.7. 5-Ethynyl-2′-deoxyuridine cell proliferation assay

We determined the cells' proliferation ability using a 5-ethynyl-2′-deoxyuridine (EdU) proliferation assay. Approximately 70 % of the A549 and h1299 cells was seeded in six-well plates. After transfection, the EdU solution (Beyotime, China) was diluted with culture medium, adjusted to the concentration recommended by the manufacturer, and then added to the cells and incubated for 2 h. The cells were then fixed with paraformaldehyde solution and washed with phosphate buffered saline (PBS, Servicebio) containing 0.3 % Triton X-100 (Solarbio). Click reaction solution was configured for EdU, and the nucleus was stained with Hoechst solution diluted in PBS and photographed under a microscope.

2.8. Wound healing assay

To photograph the same area, cells were observed for migration. we drew lines on the bottom of a well plate with a black marker, approximately every 0.5–1 cm. Lung cance cells were seeded in the labeled well plates and transfected. When they had reached approximately 90 %, the cells were transferred to serum-free medium for culture, and a 200 μL sterile pipette tip was passed gently through the cell-covered well plate and washed three times with PBS. The same streaked areas of the cells were photographed at 0 h and 24 h.

2.9. Transwell migration and invasion assay

To examine cell invasion and migration, we used a 24-well 8.0-μm transwell permeation vector (LABSELECT, China). Dilute to 12.5 % BD MatrigelTM matrix (BD Bioscience, USA) using serum-free medium was added to the Transwell chambers. A549 and H1299 cells after 48h of transfection were resuspended in serum-free medium to make a suspension (1×10^5 cells/mL). The suspension (100 μL) is then added to the perforation chamber containing the BD MatrigelTM matrix. Add an appropriate amount of 10 % complete medium to the lower chamber, place the Transwell chamber on the wells and incubate for 24 h, then fix with 4 % paraformaldehyde (Biosharp) and stain with crystal violet (Biosharp).

2.10. Western blotting assay

Transfected cells were lysed with a mixture of radioimmunoprecipitation assay (RIPA, Solarbio) buffer and phenylmethylsulphonyl fluoride (PMSF, Solarbio), and total cellular proteins were extracted. After 15 min of lysis, mix the supernatant with 5 × loading buffer and then boil for 10 min. Total protein (3 μL) and prestained protein markers (Epizyme, China) were added to 8 % sodium dodecyl sulfate polyacrylamide gel electrophoresis gels. Portions of the gels with molecular weights corresponding to those of the prestained protein labels were transferred to polyvinyl difluoride membranes, which were infiltrated with 5 % skim milk and shaken gently for 2 h. The proteins we measured were β-actin (42–43 kDa, Cat. No. 81115-1-RR, 1:2000, Proteintech, China), Vitinment (54 kDa, Cat. No. abs171412, 1:1000, Absin, China), N-cadherin (100–140 kDa, Cat. No. 22018-1-AP, 1:2000, Proteintech), E-cadherin (100–140 kDa, Cat. No. 20874-1-AP, 1:2000, Proteintech). After washing three times with TBST (Tris buffered saline with 0.1 % Tween 20, Solarbio), the membranes were shaken with primary antibody overnight at 4 °C. After 18–24 h, the membranes

were removed, washed, and incubated with secondary antibodies for 1 h.

2.11. Tumor immune cell infiltration and immune checkpoints

Tumor immune cell infiltration and immune checkpoints between the two clusters were analyzed and compared according to different expression levels of ANLN (cut-off value of 50 %). The deconvolution algorithm (CIBERSORT) was to determine the abundance of 22 types of tumor-infiltrating immune cells (TIICs) in LUAD [31]. Additionally, ssGSEA analysis was performed on 28 types of TIICs by using the GSVA package [32]. Statistical software was used to calculate the expression of seven major immune checkpoints in different ANLN clusters.

2.12. Tumor mutation burden (TMB) and therapeutic effect between the different ANLN clusters in LUAD

Tumor mutation burden (TMB) provide a visual representation of the somatic mutations and copy number alterations in different ANLN clusters [33]. Additionally, the R package "oncoPredict" was employed to compare the efficacy of chemotherapy and targeted therapy among the different ANLN clusters [34]. These analyses allow for the assessment of treatment response and potential therapeutic strategies based on the ANLN expression profile in LUAD.

2.13. Statistical analysis

The *t*-test was utilized to compare two independent samples, while the Wilcoxon rank sum test (for unpaired samples of two groups) was applied to assess the differences in clinical information among LUAD patients. ANOVA was employed to compare the differences among three or more groups. Based on the changes observed in the image, ImageJ is used for graphics calculations. Calculations were made and the data were analyzed using SPSS 26.0 and GraphPad Prism 8.0. Statistical significance was defined as $p < 0.05$ (ns, $p > 0.05$; *, $p < 0.05$; **, $p < 0.01$; ***, $p < 0.001$). Each experiment was repeated more than three times.

3. Result

3.1. Diagnostic and prognostic value of CERS6-AS1

Based on TCGA database, we found that NEDD1 was highly expressed in various cancer types (Fig. 1A). The differential analysis revealed that CERS6-AS1 is overexpressed in LUAD ($\log_2$ fold change = 1.064, $p < 0.001$, Fig. 1B). Analysis of the ROC curve and survival curve results from the TCGA database revealed that CERS6-AS1 exhibited upregulation in LUAD and displayed diagnostic and prognostic value (AUC = 0.678) (Fig. 1C and D). Univariate COX analysis showed that CERS6-AS1 (high vs. low (cutoff value was 50 %), HR = 1.516 (1.135–2.024), P = 0.005), T stage (T1 vs. T2, HR = 1.507 (1.059–2.146), P = 0.023, and T1 vs. T3+T4, HR = 1.6(1.3–1.9), P < 0.001), N stage (N0 vs. N1, HR = 2.293 (1.632–3.221), P < 0.001, and N0 vs. N2+N3, HR = 2.993 (2.057–4.354), P < 0.001), and M stage (M0 vs. M1, HR = 2.176 (1.272–3.722), P = 0.005) as independent prognostic factors for LUAD. All independent prognostic factors were included in the multivariate COX analysis, and CERS6-AS1 (high vs. low, HR = 1.425 (1.021–1.987), P < 0.037), T stage (T1 vs. T3+T4, HR = 2.650 (1.507–4.659), P < 0.001), and N stage (N0 vs. N1, HR = 2.030 (1.376–2.994), P < 0.001, and N0 vs. N2+N3, HR = 2.780 (1.813–4.262), P < 0.001) synergistically promoted LUAD progression (Fig. 1E). LUAD samples from TCGA database or clinical collection showed that CERS6-AS1 was expressed higher in LUAD tissues than in neighboring tissues (TCGA: 30 normal tissues vs. 401 LUAD tissues and clinical samples: 35 paracancerous tissues vs. 35 LUAD tissues) (Fig. 1F and G). In addition, CRES6-AS1 expression was higher in the A549, H1299, and H1975 cell lines than in the BEAS-2B normal bronchial cell line (Fig. 1H).

3.2. CERS6-AS1 silencing reduces cell proliferation

We designed three different siRNAs and used RT-qPCR to determine which siRNA with the highest knockdown efficiency for subsequent experiments, and the results showed that si-CERS6-AS1-2 had the best silencing effect (Fig. 2A). To confirm the role of CERS6-AS1 in lung cancer cell proliferation, we designed CCK-8 and EdU experiments. The CCK8 assay revealed a clear decrease in cell proliferation at 48 h after silencing CERS6-AS1, with the most pronounced effect observed at 72 h (Fig. 2B). This indicates that the suppression of CERS6-AS1 has a notable impact on reducing cell proliferation in lung cancer. Additionally, the EdU assay demonstrated that CERS6-AS1 knockdown significantly decreased the number of proliferating cells. Taken together, these findings underscore the role of CERS6-AS1 in promoting lung cancer cell proliferation (Fig. 2C).

3.3. CERS6-AS1 downregulation affects cell migration, invasion, and EMT progression

In the wound healing assay, the migration rate of si-CERS6-AS1-2 transfected A549 and H1299 cells decreased after 24 h (Fig. 3A). The transwell assays showed that CERS6-AS1 silencing significantly inhibited cell migration and invasion (Fig. 3B). Western blot (WB) showed that N-cadherin and Vimentin expression decreased after CERS6-AS1 silencing, while E-cadherin expression increased (Fig. 3C). Thus, CERS6-AS1 silencing affected lung cancer cell migration, invasion, and EMT.

3.4. CERS6-AS1 affects the progression of LUAD by sponging of miR-424-5p

The results of the five miRNAs that can be sponge adsorbed by CERS6-AS1 are shown in Fig. 4A. In lung cancer cell lines that were transfected with si-CERS6-AS1-2, there was a significant increase in the expression of miR-424-5p (Fig. 4B). RT-qPCR showed low miR-424-5p in LUAD tissues and lung cancer cell lines (Fig. 4C and D). In addition, miR-424-5p expression levels regulated by miR-424-5p-mimic and miR-mimic-NC were verified in A549 and H1299 cells (Fig. 4E). The wild-type CERS6-AS1 and miR-424-5p have a specific sponge structure, and the luciferase activity of wild-type CERS6-AS1 containing miR-424-5p-mimic was lower than miR-mimic-NC, while no significant difference in this activity was observed on mutant CERS6-AS1 (Fig. 4F).

3.5. The miR-424-5p inhibitor partially rescues the downregulation of CERS6-AS1 to cell proliferation

CCK8 assays showed that miR-424-5p inhibitors partially rescued the proliferation of si-CERS6-AS1-2 transfected lung cancer cells. (Fig. 5A). In addition, EdU assays demonstrated that the EdU positivity observed in the si-CERS6-AS1-2 and miR-424-5p inhibitor cotransfection group was higher than in the si-CERS6-AS1-2 group (Fig. 5B). This reflects the ability of CERS6-AS1 to regulate the proliferation of A549 and H1299 cells through sponge adsorption of miR-424-5p.

3.6. The miR-424-5p inhibitor partially rescues the downregulation of CERS6-AS1 to cell migration, invasion, and EMT

Previous conclusions indicate that si-CERS6-AS1-2 transfection inhibits cell migration in wound healing assays, increasing again with the addition of miR-424-5p inhibitor cotransfection (Fig. 6A). The transwell assay showed that the cell migration and invasion abilities were better in the co-transfection group than in the si-CERS6-AS1-2 group, but it did not exceed those of the si-NC groups (Fig. 6B). WB results showed that

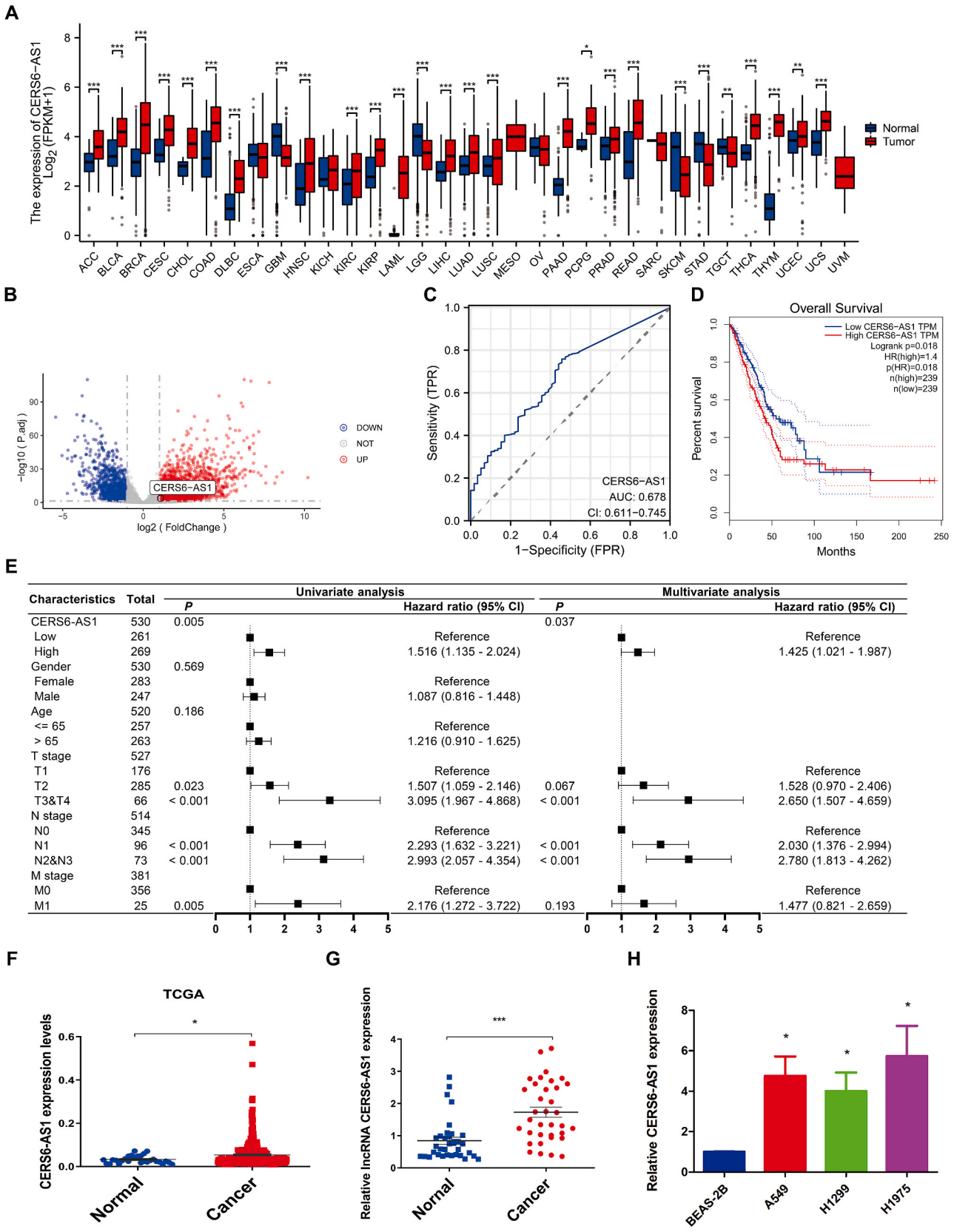

Fig. 1. Bioinformatics analysis and verification of CERS6-AS1. (A) Pan-cancer analysis of CERS6-AS1. (B) The volcano map made by TCGA database, and lncRNA CERS6-AS1 was highly expressed in most lung cancer tissues (log2FoldChange = 1.064, $p < 0.001$). (C) ROC curve analysis of CERS6-AS1 in the TCGA database. (D) Kaplan-Meier survival curves imply that patients with high CERS6-AS1 expression have a low overall survival. (E) Univariate COX analysis of clinical features and CERS6-AS1 in LUAD, and Multivariate COX analysis of independent prognostic factors in LUAD. (F) TCGA database showed higher expression in LUAD. (G) RT-qPCR results were consistent with the TCGA database results. (H) CERS6 AS1 showed the same results in lung cancer cell lines as in LUAD tissues.

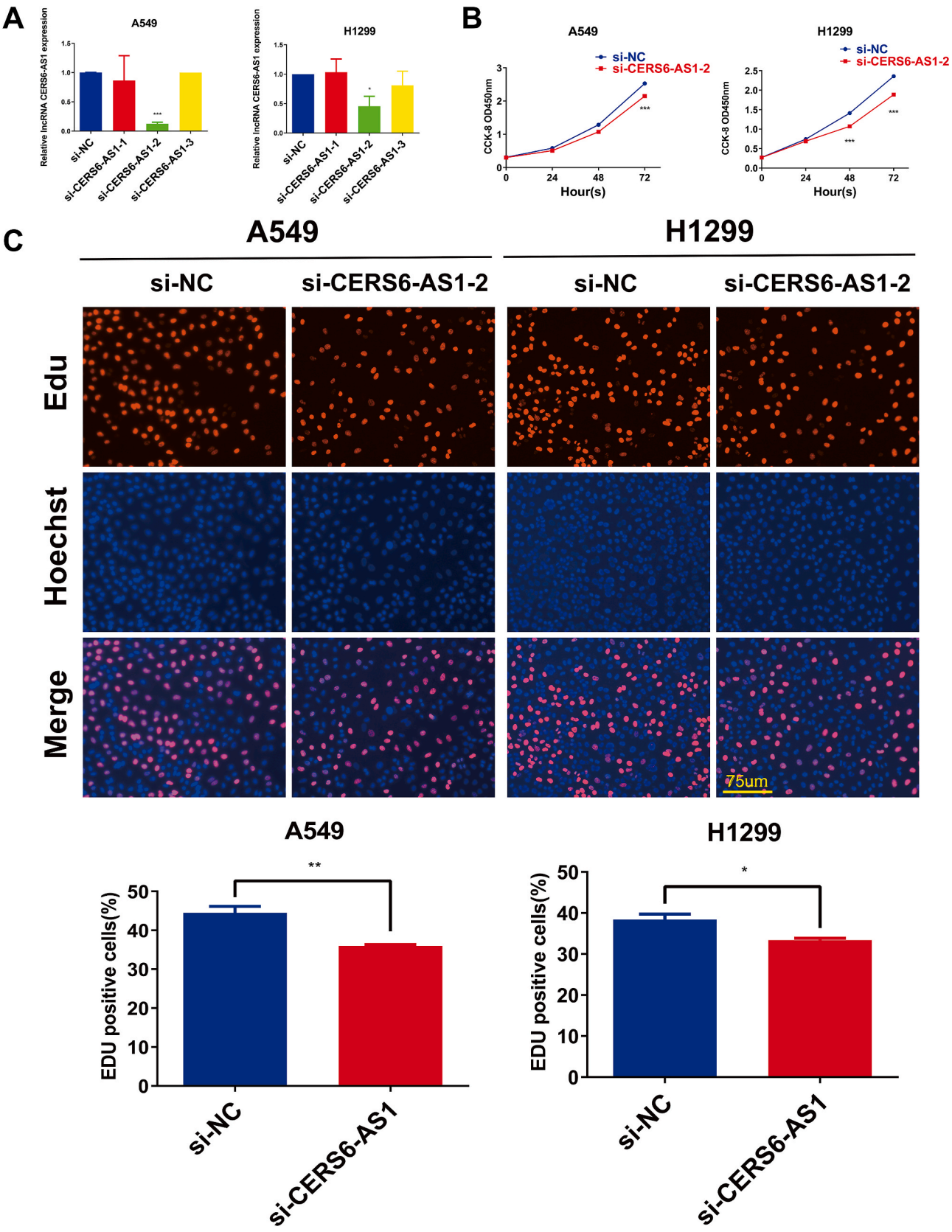

Fig. 2. CERS6-AS1 silencing reduces cell proliferation. (A) The siRNAs were transfected into A549 and H1299, and the silencing efficiency was evaluated by RT-qPCR. (B) The CCK8 assay showed a reduced proliferation rate of A549 and H1299 cells after knocking down CERS6-AS1 compared to the negative control group (NC group). (C) After knocking down CERS6-AS1, the EDU staining rate of A549 and H1299 cells was lower compared to the NC group.

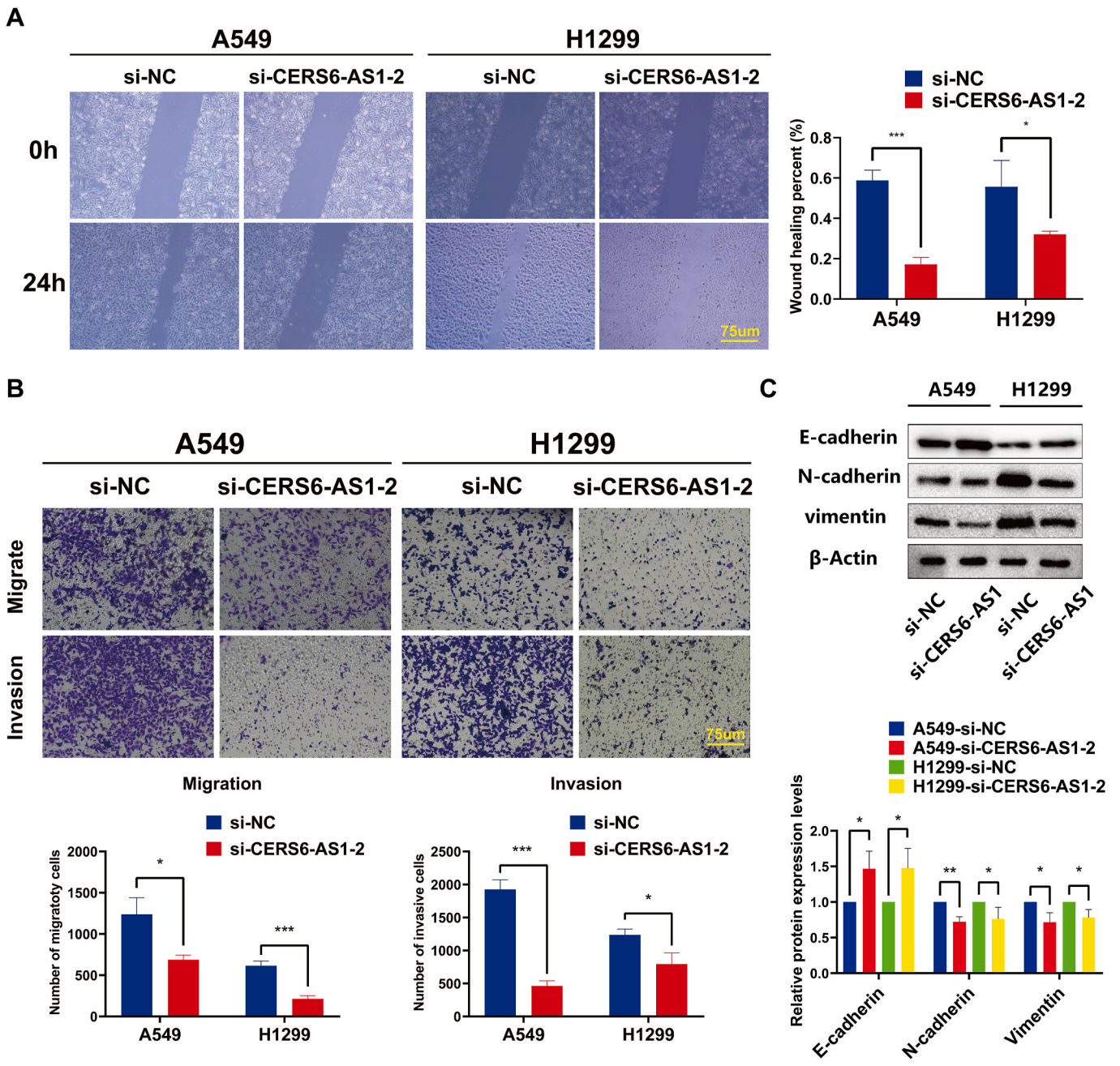

Fig. 3. CERS6-AS1 downregulation affects cell migration, invasion, and EMT progression. (A) Wound healing assay showed the migration ability of the different treated cells. (B) After silencing CERS6-AS1, the invasion and migration abilities of the cells were less than those of the NC group. (C) The Western blot technique was used to assess the capacity of cells for epithelial-mesenchymal transformation.

co-transfection reversed the CERS6-AS1 knockdown induced effect on EMT to a certain extent (Fig. 6C).

3.7. ANLN may be a target of CERS6-AS1/miR-424-5p

Using database prediction and intersection methods, a total of 26 potential target genes for miR-424-5p were identified (Fig. 7A). The ceRNA network of the CERS6-AS1/miR-424-5p axis (Fig. 7B). The proteins expressed by these genes are closely related to each other (Fig. 7C). Nodal proteins in protein interaction analysis were analyzed for functional enrichment (FASN, FGF2, MYB, WEE1, KIF23, FGFR1, VEGFA, MAP2K1, CHEK1, CCND1, SOCS6, CDC25A, PTCH1, CUL2, ANLN, CCND3, CDK6, CDC14A), and it was found that these proteins were mainly localized to the nucleus or cytoskeleton and were involved in the regulation of cell cycle and cell isolation ($p < 0.01$, Fig. 7D). Anillin (ANLN) is mainly distributed in the nucleus and cytoskeleton, interacting with major cytoskeletal structures, such as actin filament, microtubules, and septal polymers, involved in regulating cell division [15]. Our results found that ANLN expression was significantly upregulated in LUAD (Fig. 7E). Its ROC curve area is 0.9805, which has good diagnostic significance (Fig. 7F). Meanwhile, high ANLN expression was associated with a poor prognosis in patients with LUAD ($p < 0.001$) (Fig. 7G). Relative expression of ANLN was increased in lung cancer cell lines (Fig. 7H). In addition, we also verified the expression level of ANLN regulated by si-CERS6-AS1 group and si-CERS6-AS1 and miR-424-5p inhibitor co-transfection group in A549 and H1299 cells. The results showed that CERS6-AS1 knockout inhibited the expression of ANLN in lung cancer cells, while miR-424-5p inhibitor partially restored the

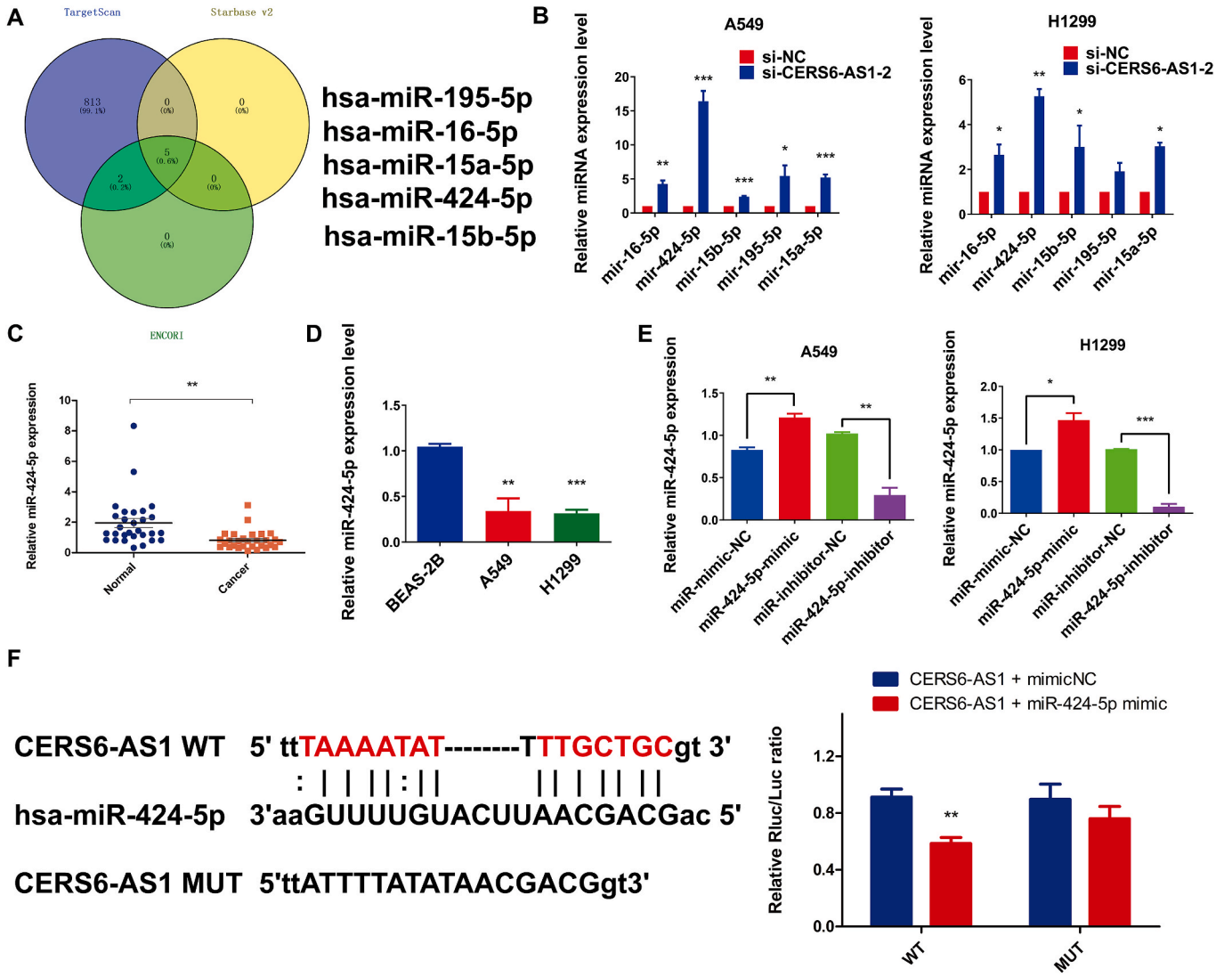

Fig. 4. CERS6-AS1 affects the progression of LUAD by sponging miR-424-5p. (A) Target genes were screened using the database. (B) The expression levels of miRNAs in the transfected lung cancer cell lines were screened. (C) The expression of miR-424-5p was decreased in lung cancer tissues. (D) The expression of miR-424-5p was decreased in lung cancer cell lines. (E) Transfection efficiency of miR-424-5p mimic and miR-424-5p inhibitor. (F) Plasmid construction and verification of target gene relationships and luciferase experiments.

expression of ANLN in CERS6-AS1 knockout cells (Fig. 7I). The binding sites of miR-424-5p and ANLN were predicted by ENCORI website and verified by dual luciferase reporter gene assay. The results showed that the relative luciferase activity of ANLN transfected with miR-424-5p mimic and wild type was lower than that of mimicNC and wild type ANLN. However, the relative luciferase activity of mutant ANLN did not change (Fig. 7J).

3.8. Based on tumor immune infiltration and tumor mutation burden, the immune checkpoint and drug sensitivity characteristics of ANLN

We use the cibersort algorithm and ssGSEA to assess the effect of ANLN-associated tumor immune infiltration on immune checkpoints. In high ANLN cluster, infiltration of memory B cells, resting memory CD4 T cells, regulatory T cells, monocytes, resting dendritic cells, resting mast cells in LUAD increased, while activated memory CD4 T cells, resting natural killer cells, M0 and M1 macrophages decreased. (Fig. 8A). Single-sample gene set enrichment analysis (ssGSEA) showed increased infiltration of CD4 T cells, central memory CD8 T cells, effector memory CD4 T, γδT cells, memory B cells, natural killer T cells, neutrophils, type 2 helper T cells activated in high ANLN cluster, while naïve B cells, activated B cells, eosinophils, naïve dendritic cells, plasmacytoid dendritic cells, macrophages, mast cells, monocytes, follicular helper T cells, Type 17 helper T cell infiltration is reduced. (Fig. 8B). To observe the effect of ANLN expression on tumor mutation burden, we examined data from 250 patients with high ANLN expression and 249 patients with low ANLN expression in TCGA, with oncogene mutations occurring in 95.2 % of patients in high ANLN clusters and 90.76 % in low ANLN clusters (Fig. 8C). Meanwhile, the mutations per million base pairs unit (muts/Mb) was significantly higher in the high ANLN cluster than in the low ANLN cluster (Fig. 8D). The major regulatory targets (PD1, CD274, PDCD1LG2 and LAG3) had significantly greater expression in the high ANLN cluster than in the low ANLN cluster (Fig. 8E). In addition, we examined the relevance of ANLN with common first-line therapeutic drugs, including cisplatin, paclitaxel, docetaxel, erlotinib, and gefitinib, with high ANLN expression having a lower half-maximal inhibitory concentration (IC50) relative to low ANLN expression, suggesting that high ANLN results in better therapeutic outcomes (Fig. 8F).

4. Discussion

Lung cancer, being one of the most malignant tumor diseases

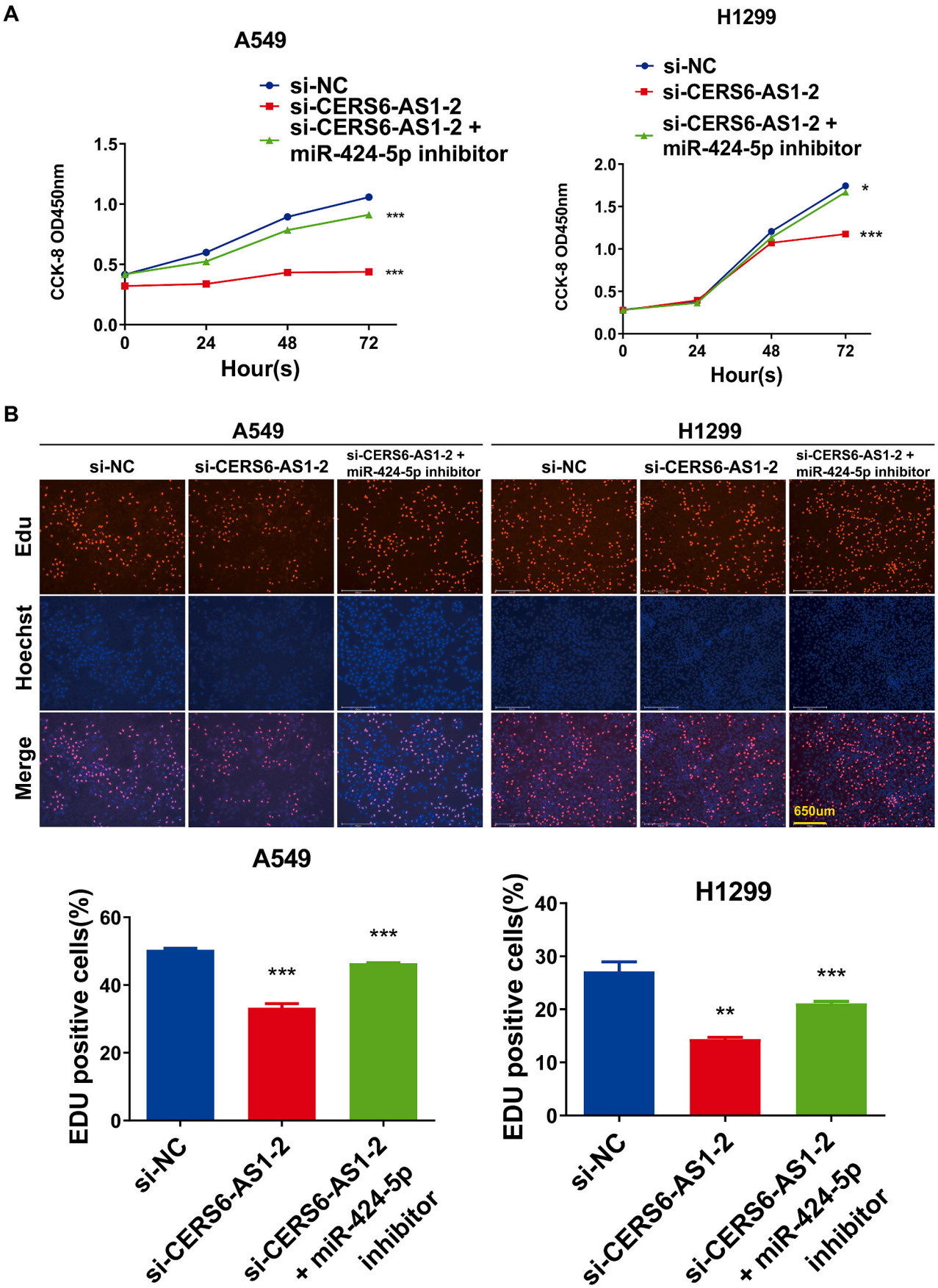

Fig. 5. The miR-424-5p inhibitor partially rescues the downregulation of CERS6-AS1 to cell proliferation. (A and B) miR-424-5p inhibitor could partially eliminate the effect of silencing CERS6-AS1 on the proliferation of LUAD cells.

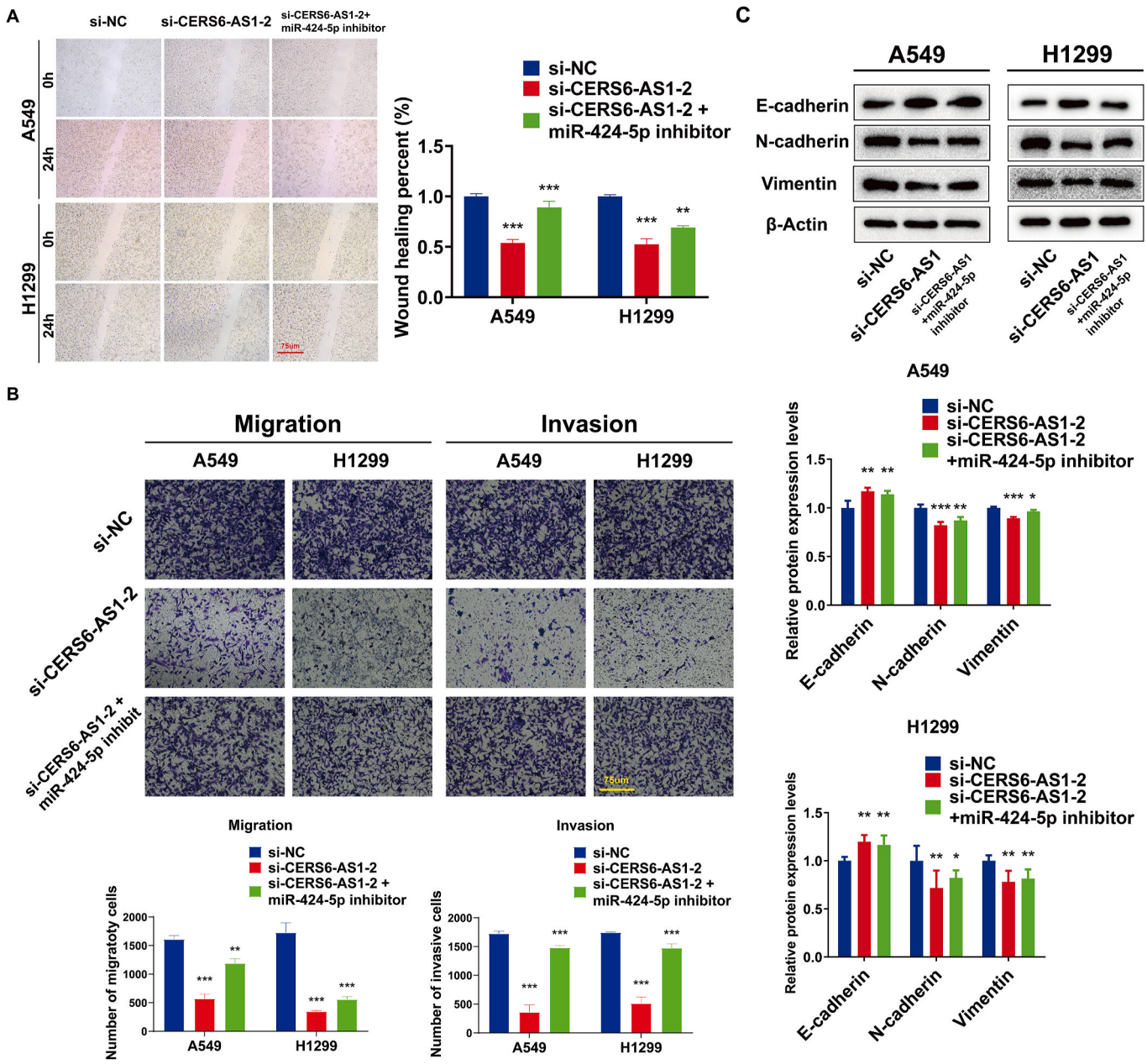

Fig. 6. The miR-424-5p inhibitor partially rescues the downregulation of CERS6-AS1 to cell migration, invasion, and EMT. (A) Wound healing assay shows miR-424-5p inhibitor treatment of CERS6-AS1 knockdown cell recovery partial migration ability. (B) Transwell assay shows miR-424-5p inhibitor treatment of CERS6-AS1 knockdown cell recovery partial migration and invasion ability. (C) The addition of miR-424-5p inhibitors resulted in alterations in the expression levels of EMT proteins.

globally, has experienced a decline in developed countries due to reduced smoking rates and the widespread adoption of early low-dose CT screening. However, in less developed regions, the number of new cases and mortality rates of lung cancer have not yet reached their peak [2,35]. The highly malignant nature of lung cancer, along with its rapid early progression and the limited effectiveness of available treatment options, contribute to its status as the deadliest oncology disease globally. Currently, early surgical radical treatment is recommended for non-metastatic lung cancer, with the option of postoperative chemotherapy and targeted therapy if the tumor progresses, to extend patient survival. However, there is still no consensus on the optimal first-line treatment for advanced lung cancer, and the selection of treatment largely depends on the tumor's pathological type. Consequently, there is an urgent need for new treatment strategies in this population [2]. The endogenous regulation of oncogene/cancer suppressor gene expression through the competing endogenous RNA (ceRNA) network holds promise as a novel therapeutic approach, because disrupting abnormal ceRNA networks or interfering ceRNA networks will affect the expression of downstream target genes [8]. In our study, we have identified CERS6-AS1 as a cancer-promoting lncRNA that is highly expressed and linked to poor prognosis in cases of lung adenocarcinoma. To investigate the impact of CERS6-AS1, we conducted cytological experiments involving knockdown of CERS6-AS1. Our findings revealed that the knockdown group exhibited decreased cell proliferation, invasion, migration, and epithelial-mesenchymal transition (EMT) capacity. Our findings are consistent with previous studies which have reported a direct association between high expression of CERS6-AS1 and poor prognosis in various other types of cancer, including breast, colorectal, gastric, thyroid, hepatocellular carcinoma, and pancreatic cancer [36]. These results strongly suggest that CERS6-AS1 plays a role in promoting

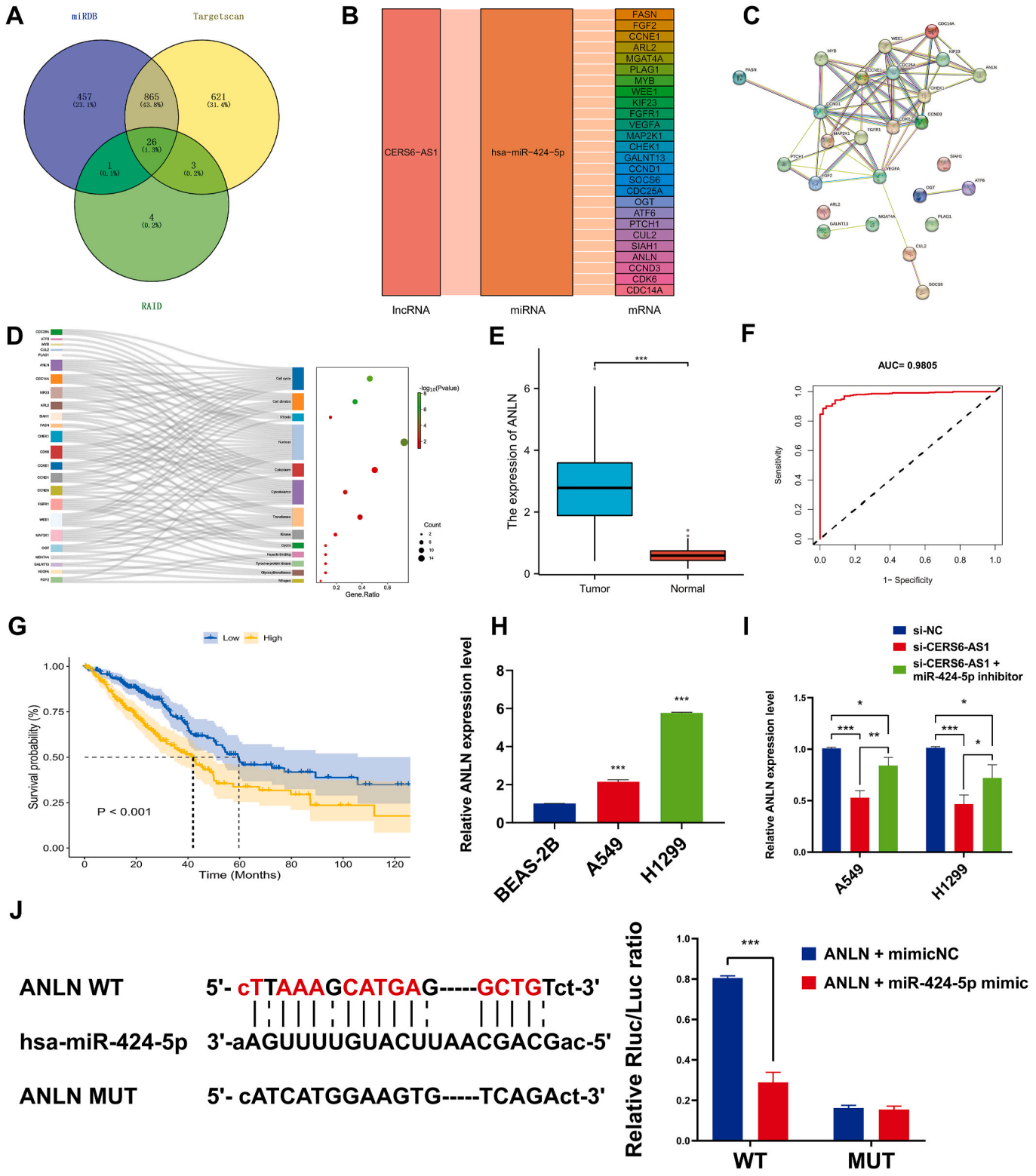

Fig. 7. ANLN may be a target of CERS6-AS1/miR-424-5p. (A) The common target genes of miR-424-5p screened by the three databases. (B) The ceRNA network of the CERS6-AS1/miR-424-5p axis. (C) Protein-protein interaction network constructed by 26 target genes. (D) Through functional enrichment analysis of the node proteins, it was determined that these proteins are mainly localized to the nucleus or cytoskeleton. Additionally, they play a role in regulating cell cycle and cell division processes. (E) ANLN expression was significantly upregulated in LUAD. (F) The ROC curve analysis yielded an area under the curve (AUC) of 0.9805, indicating that ANLN holds significant diagnostic value in predicting LUAD. (G) High ANLN expression was found to be associated with a poor prognosis in patients diagnosed with LUAD. (H) Relative expression of ANLN in lung cancer cell lines. (I) CERS6-AS1 knockout inhibited the expression of ANLN in lung cancer cells, while miR-424-5p inhibitor partially restored the expression of ANLN in CERS6-AS1 knockout cells. (J) Validation of the targeting relationship between ANLN and miR-424-5p and luciferase experiment.

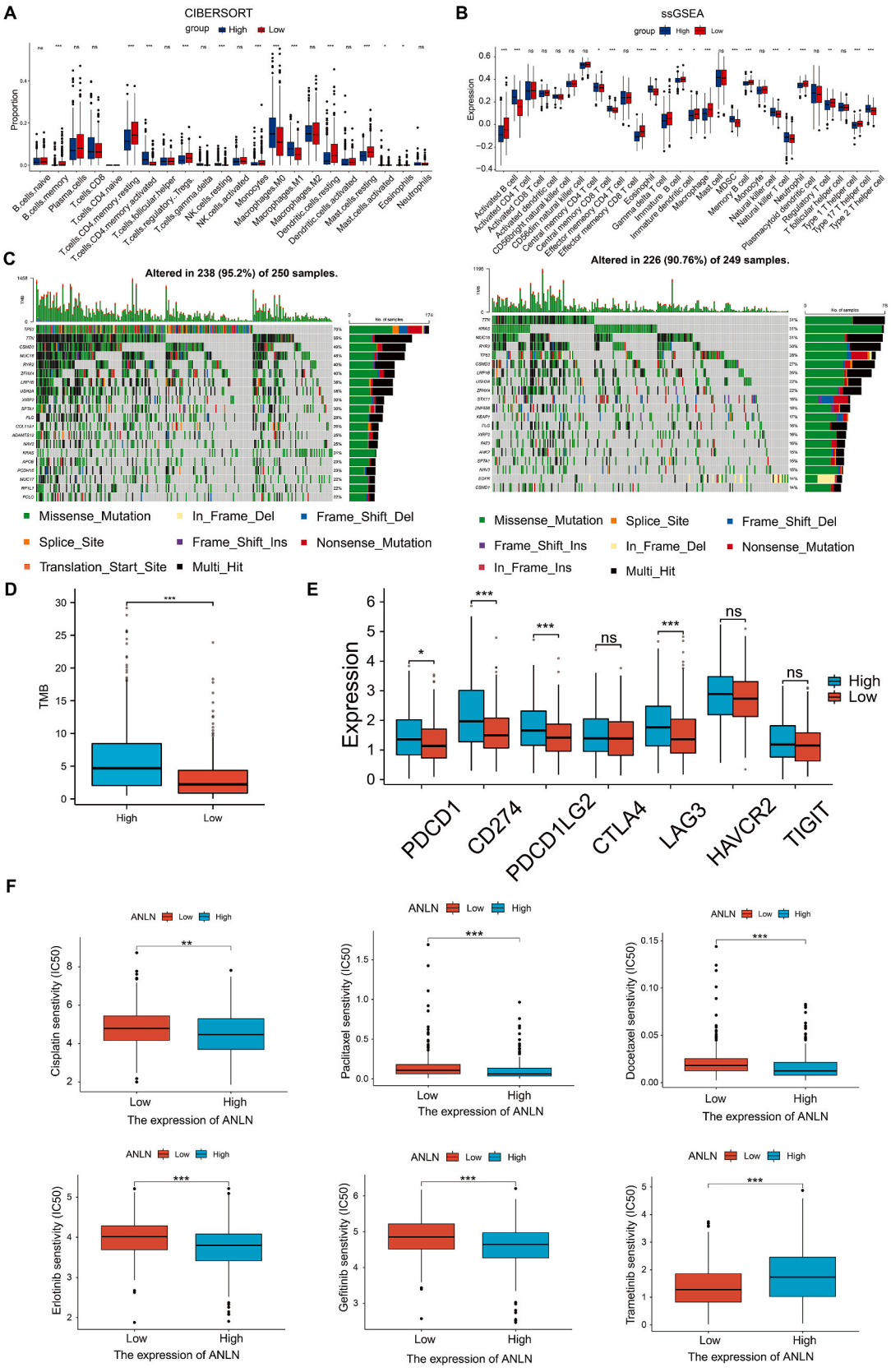

Fig. 8. The tumor immune infiltration, tumor mutation burden, immune checkpoint, and drug sensitivity characteristics of ANLN. (A and B) Tumor immune infiltrating cells affected by ANLN expression were measured using the cibersort algorithm and ssGSEA. (C and D) The correlation between ANLN expression and tumor mutational burden was examined. (E) The impact of ANLN expression on immune checkpoint levels was examined. (F) Drug sensitivity is influenced by ANLN expression.

the biological behavior of LUAD cells.

To investigate the mechanisms underlying the promotion of LUAD progression by CERS6-AS1, we employed online databases to predict potential miRNAs that could interact with CERS6-AS1. Subsequently, we identified five miRNAs (miR-195-5p, miR-16-5p, miR-15b-5p, miR-424-5p, miR-15a-5p) that exhibited a high likelihood of binding to and interacting with CERS6-AS1. Through RT-qPCR validation, we observed a significant increase in the expression of miR-424-5p in CERS6-AS1 knockdown A549 and H1299 cells. Our analysis further confirmed that miR-424-5p displayed low expression in both LUAD clinical samples and lung cancer cell lines. Furthermore, luciferase experiments and the application of both miR-424-5p mimics and inhibitors provided conclusive evidence that CERS6-AS1 functions as a sponge for miR-424-5p. According to Xuan et al., a comprehensive summary of miR-424-5p regulation and function in cancer, miR-424-5p is frequently recognized as a tumor suppressor gene with involvement in various human cancers [13]. Teng et al. discovered that the lncRNA MYLK-AS1 promotes tumor progression and angiogenesis in hepatocellular carcinoma by targeting the miR-424-5p/E2F7 axis and activating the VEGFR-2 signaling pathway [37]. Furthermore, Narges Dastmalchi et al. reported that miR-424-5p acts as a potential tumor suppressor miRNA in breast cancer. It modulates cell growth, apoptosis, and T cell-associated immune responses by targeting PD-L1 and its downstream mediators [38]. To further investigate the role of miR-424-5p, we incorporated miR-424-5p inhibitors as an additional control group in conjunction with the CERS6-AS1 knockdown group. Based on our experimental findings, the introduction of miR-424-5p inhibitors during the co-transfection of si-CERS6-AS1-2 leads to a partial restoration of CERS6-AS1 silencing. Consequently, we observed a noticeable rescue of cell proliferation, invasion, migration, and EMT. These results provide compelling evidence to support the idea that CERS6-AS1 promotes the proliferation of LUAD cells by sponging miR-424-5p.

In our study, we aimed to determine the target gene for CERS6-AS1/miR-424-5p. To achieve this, we utilized a widely used ceRNA network prediction database to identify 26 potential downstream genes. Subsequently, we performed a comprehensive analysis by considering protein-protein interaction (PPI) networks and conducting functional enrichment analysis. Through this process, we identified that the Anillin (ANLN) protein acts as a central node in the PPI network. ANLN is primarily localized in the nucleus and cytoskeleton, which is an essential actin-binding protein that plays a crucial role in regulating the cell cycle and cell division [39]. Our findings suggest that CERS6-AS1 promotes the proliferation of LUAD cells through the upregulation of ANLN by sponging miR-424-5p. Notably, distribution of ANLN varies at different phases of the cell cycle. During the interphase, the ANLN protein is localized only in the nucleus, whereas it becomes cytoplasmic during mitosis [16]. This is since ANLN contains domains associated with cleavage furrow formation during cell division, including the actin binding domain and the pleckstrin homology (PH) domain. The PH domain at the C-terminal of ANLN is required to mediate protein recruitment to the plasma membrane. When ANLN is released from the nucleus during mitosis, co-targets the cellular cortex with septin, which has a similar PH domain, to form the ANLN/septin complex. Meanwhile, through the actin binding domain located at the N-terminal, ANLN may function together with the septin, actin, and myosin II during the assembly and ingression of the cleavage furrow [40]. Our results suggest that the increased expression of ANLN in LUAD is associated with poor prognosis and can be used as a good prognostic marker for LUAD. Li et al. found that ANLN knockdown in A549 and H1299 cells would lead to activation of pyroptosis-associated pathways and thus inhibit the progression of LUAD [16]. Furthermore, targeting ANLN in several other ceRNA regulatory networks has been found to affect the tumor immune microenvironment and enhance tumor multidrug resistance [41–43]. Therefore, ANLN expression has been closely linked to tumor immune cell infiltration and the efficacy of immune checkpoint therapy [44]. Building upon these findings, we revisited the role of ANLN in the prognosis of LUAD and its potential as an immunobiomarker.

The tumor microenvironment consists of both tumor cells and non-tumor cell components, and the ongoing interaction between tumor-infiltrating immune cells and the tumor microenvironment plays a critical role in tumor initiation, progression, metastasis, and response to treatment [45]. Therefore, immune checkpoints involved in regulating tumor immune cell infiltration and immune tolerance in the tumor microenvironment have garnered significant research and clinical attention as potential therapeutic targets in cancer treatment [46]. Despite variations in the correlation calculation methods used to assess the relationship between ANLN and tumor-infiltrating immune cells in LUAD, the conclusions drawn from both approaches remain consistent. Specifically, high ANLN expression clusters are associated with increased infiltration of resting anti-tumor immune cells and immunosuppressive cells, along with decreased presence of activated anti-tumor immune cells and innate immune cells. These findings suggest that ANLN may be linked to poor immune responsiveness. Cell resting state refers to a specific cellular state in which cells undergo reversible cell cycle arrest in response to environmental stimuli. In the absence of activation signals, T cells enter a resting state characterized by reduced proliferation and preservation of the essential metabolic rate for survival. Subsequently, upon activation signals from the T cell receptor and co-stimulation, T cells exit the quiescent state and progress into the clonal expansion and differentiation phase, exerting specific immune effects [47]. Effector CD4 T cells contribute to the antitumor response indirectly by boosting the antitumor activity of immune cells and producing inflammatory cytokines [48]. Helper CD4 T cells can be classified into different subsets, including Th1, Th2, Th17, and regulatory T cells (Tregs). In high ANLN clusters, there is an increase in tumor invasion by Th2 and Tregs cells, while the invasion by Th17 cells is reduced. Th2 cells secrete IL-10, which helps inhibit inflammation. Tregs cells, on the other hand, promote tumor development. Th17 cells indirectly contribute to anti-tumor effects by promoting T cell recruitment to tumors and activating CD8 T cells [49,50]. Consistent with the findings of Yao et al., we found that ANLN aggravates tumor progression by regulating T-cell-mediated cytotoxicity in the tumor microenvironment [41]. On the other hand, decreased infiltration of macrophages, mast cells, and dendritic cells, which are essential for anti-tumor activity and antigen presentation, further inhibited T cell activation. Furthermore, we investigated the correlation between ANLN expression levels and seven immune checkpoints, namely PDCD1, CD274, PDCD1LG2, CTLA4, LAG3, HAVCR2, and TIGIT. Our results align with previous findings, indicating abnormal upregulation of PDCD1, CD274, PDCD1LG2, and LAG3 in high ANLN clusters. This suggests that low immunoreactivity, potentially regulated by immune checkpoints, is associated with immune tolerance, ultimately promoting tumor growth and migration by dampening the anti-tumor response [51–53]. In conclusion, ANLN, functioning as an oncogene, plays a crucial role in modulating the immune infiltration and immune checkpoint in the tumor microenvironment. Consequently, the upregulation of ANLN, facilitated by the sponge effect of CERS6-AS1 on miR-424-5p, amplifies the cancer-promoting function, leading to increased proliferation, migration, invasion, epithelial-mesenchymal transformation, and immune evasion of LUAD cells.

In terms of gene mutation analysis, high ANLN clusters displayed a higher tumor mutational burden (TMB) in comparison to low ANLN clusters. This discrepancy in TMB has implications in two aspects. Firstly, TMB can influence a patient's response to immune checkpoint inhibitors (ICIs) by modulating the production of immunogenic peptides. Secondly, identification of mutated oncogenes can guide the selection of appropriate drugs for treatment purposes [54]. The inhibitory gene TP53 is the most mutated gene in human cancer and is also a well-known undruggable target [55]. Although there are no recommended drugs for TP53 mutations, our study shows that TP53 mutation rates of up to 70 % in high ANLN clusters mean that LUAD patients are more likely to benefit from targeted therapies. Therefore, we further

analyzed the sensitivity of ANLN to chemotherapy and targeted therapy, and the lower the semi-inhibitory concentration (IC50), the higher the drug sensitivity. High ANLN clusters have lower IC50 values in cisplatin, paclitaxel, docetaxel, erlotinib, and gefitinib, while trametinib in NSCLC BRAF V600-positive patients has higher IC50 values, which may be related to higher KRAS mutation rates in low ANLN clusters. For this reason, chemotherapy or single-agent targeted therapy is still the first-line treatment of choice for advanced LUAD patients with high expression of ANLN with positive driver genes or negative driver genes. However, when patients develop paclitaxel resistance (PTX resistance) or genetic mutations, targeting the CERS6-AS1/miR-424-5p/ANLN regulatory axis combined immune checkpoint inhibitors to treat LUAD with high ANLN expression may offer a new treatment option.

5. Conclusion

We analyzed that upregulation of lncRNA CERS6-AS1 in LUAD was associated with poor prognosis in patients based on the TCGA database. Inhibition of CERS6-AS1 expression in LUAD cell lines can reduce cell proliferation, invasion, migration, and epithelial-mesenchymal transformation. We further hypothesized that CERS6-AS1 might target the miR-424-5p/ANLN axis to regulate LUAD progression and immune evasion. To validate our hypothesis, we introduced miR-424-5p inhibitors into cells that had been knocked down for CERS6-AS1. Interestingly, we observed that miR-424-5p inhibitor enhanced cell proliferation, invasion, migration, and epithelial-mesenchymal transformation compared to cells that only CERS6-AS1 knockdown, as well as increased expression of ANLN. In addition, ANLN, as an oncogene, is expected to be a valuable prognostic and immune biomarker due to its role in regulating cell division, promoting cell proliferation, and playing a crucial role in regulating immune infiltration and immune check points in the tumor microenvironment. Considering these insights, targeting the CERS6-AS1/miR-424-5p/ANLN regulatory axis combined immune checkpoint inhibitors is expected to provide a novel and effective treatment for advanced LUAD with PTX resistance or driver gene mutations.

Contributions

Ting Zhuo: Conceptualization, Validation and Writing - original draft. Zuotao Wu: Methodology, Investigation and Validation. Chuyi Yang: Methodolog and Investigation. Zihao Li and Hongyu Huang: Methodology and Software. Jinyan Gan and Nijiao Li: Data curation and Resources. Xiaohong Li and Jueqi Lyu: Formal analysis. Shouming Qin and Yanbin Wu: Writing – review & editing, Supervision, Funding acquisition, Project administration.

Funding

Shouming Qin is supported by the research project funded by Guangxi Health Commission [Approval No. Z20180975]. Yanbin Wu is supported by Guangxi Appropriate Medical Health Technology Promotion Project [Approval No. S2020026].

Ethical approval

The study was conducted in accordance with the Declaration of Helsinki and approved by the Ethics Committee of the First Affiliated Hospital of Guangxi Medical University (Review acceptance No. 2023-E343-01).

Consent to participate

Informed consent was obtained from all participants involved in the study.

Availability of data and materials

The data are available from the corresponding author upon reasonable request.

CRediT authorship contribution statement

Zhuo Ting: Conceptualization, Validation, Writing – original draft. **Zuotao Wu:** Investigation, Methodology, Validation. **Chuyi Yang:** Investigation, Methodology. **Zihao Li:** Methodology, Software. **Hongyu Huang:** Methodology, Software. **Jinyan Gan:** Data curation, Resources. **Nijiao Li:** Data curation, Resources. **Xiaohong Li:** Formal analysis. **Jueqi Lyu:** Formal analysis. **Yanbin Wu:** Funding acquisition, Project administration, Supervision, Writing – review & editing. **Shouming Qin:** Funding acquisition, Project administration, Supervision, Writing – review & editing.

Declaration of competing interest

The authors declare that they have no known competing financial interests or personal relationships that could have appeared to influence the work reported in this paper.

Appendix A. Supplementary data

Supplementary data to this article can be found online at https://doi.org/10.1016/j.ncrna.2023.11.013.

References

[1] M.A. Zaimy, N. Saffarzadeh, A. Mohammadi, H. Pourghadamyari, P. Izadi, A. Sarli, L.K. Moghaddam, S.R. Pascheparis, H. Azizi, S. Torkamandi, et al., New methods in the diagnosis of cancer and gene therapy of cancer based on nanoparticles, Cancer Gene Ther. 24 (2017) 233–243, https://doi.org/10.1038/cgt.2017.16.
[2] R.L. Siegel, K.D. Miller, N.S. Wagle, A. Jemal, Cancer statistics, 2023, Ca-Cancer J Clin 73 (2023) 17–48, https://doi.org/10.3322/caac.21763.
[3] S.L. Wood, M. Pernemalm, P.A. Crosbie, A.D. Whetton, The role of the tumor-microenvironment in lung cancer-metastasis and its relationship to potential therapeutic targets, Cancer Treat Rev. 40 (2014) 558–566, https://doi.org/10.1016/j.ctrv.2013.10.001.
[4] K. Yoneda, N. Imanishi, Y. Ichiki, F. Tanaka, Immune checkpoint inhibitors (ICIs) in non-small cell lung cancer (NSCLC), J. UOEH 40 (2018) 173–189, https://doi.org/10.7888/juoeh.40.173.
[5] D.F. Quail, J.A. Joyce, Microenvironmental regulation of tumor progression and metastasis, Nat Med 19 (2013) 1423–1437, https://doi.org/10.1038/nm.3394.
[6] M.J. Al-Imam, U.A.R. Hussein, F.F. Sead, A.M.A. Faqri, S.M. Mekkey, A.J. Khazel, H.A. Almashhadani, The interactions between DNA methylation machinery and long non-coding RNAs in tumor progression and drug resistance, DNA Repair (2023) 128. ARTN 10352610.1016/j.dnarep.2023.103526.
[7] J.S. Mattick, Non-coding RNAs: the architects of eukaryotic complexity, EMBO Rep. 2 (2001) 986–991, https://doi.org/10.1093/embo-reports/kve230.
[8] L. Salmena, L. Poliseno, Y. Tay, L. Kats, P.P. Pandolfi, A ceRNA hypothesis: the Rosetta stone of a hidden RNA language? Cell 146 (2011) 353–358, https://doi.org/10.1016/j.cell.2011.07.014.
[9] L. Yan, K. Li, Z.Y. Feng, Y.Z.H. Zhang, R.R. Han, J.Z. Ma, J.L. Zhang, X. Wu, H. J. Liu, Y.X. Jiang, et al., lncRNA CERS6-AS1 as ceRNA promote cell proliferation of breast cancer by sponging miR-125a-5p to upregulate BAP1 expression, Mol Carcinogen 59 (2020) 1199–1208, https://doi.org/10.1002/mc.23249.
[10] J.J. Zhang, W.Y. Lou, A key mRNA-miRNA-lncRNA competing endogenous RNA triple sub-network linked to diagnosis and prognosis of hepatocellular carcinoma, Front. Oncol. 10 (2020). ARTN 34010.3389/fonc.2020.00340.
[11] J. Xu, J. Wang, Z.W. He, P. Chen, X.Y. Jiang, Y.K. Chen, X.Y. Liu, J.X. Jiang, LncRNA CERS6-AS1 promotes proliferation and metastasis through the upregulation of YWHAG and activation of ERK signaling in pancreatic cancer, Cell Death Dis. 12 (2021). ARTN 64810.1038/s41419-021-03921-3.
[12] T.X. Lu, Rothenberg, M.E. MicroRNA, J Allergy Clin Immun 141 (2018) 1202–1207, https://doi.org/10.1016/j.jaci.2017.08.034.
[13] J.Y. Xuan, Y.X. Liu, X.P. Zeng, H.M. Wang, Sequence Requirements for miR-424-5p regulating and function in cancers, Int. J. Mol. Sci. (2022) 23. ARTN 403710.3390/ijms23074037.
[14] Y. Li, C.M. Zhang, Z.Y. Zhao, CircSLCO3A1 depletion ameliorates lipopolysaccharide-induced inflammation and apoptosis of human pulmonary alveolar epithelial cells through the miR-424-5p/HMGB3 pathway, Mol Cell Toxicol (2023), https://doi.org/10.1007/s13273-023-00341-6.
[15] N.G. Naydenov, J.E. Koblinski, A.I. Ivanov, Anillin is an emerging regulator of tumorigenesis, acting as a cortical cytoskeletal scaffold and a nuclear modulator of

cancer cell differentiation, Cell. Mol. Life Sci. 78 (2021) 621–633, https://doi.org/10.1007/s00018-020-03605-9.
[16] L. Sheng, Y.H. Kang, D.L. Chen, L.Y. Shi, Knockdown of ANLN inhibits the progression of lung adenocarcinoma via pyroptosis activation, Mol. Med. Rep. 28 (2023). ARTN 17710.3892/mmr.2023.13064.
[17] H.X. Jia, F. Yu, B.Y. Li, Z.Y. Gao, Actin-binding protein Anillin promotes the progression of gastric cancer in vitro and in mice, J. Clin. Lab. Anal. 35 (2021). ARTN e2363510.1002/jcla.23635.
[18] D.D. Wang, N.G. Naydenov, M.G. Dozmorov, J.E. Koblinski, A.I. Ivanov, Anillin regulates breast cancer cell migration, growth, and metastasis by non-canonical mechanisms involving control of cell stemness and differentiation, Breast Cancer Res. 22 (2020). ARTN 310.1186/s13058-019-1241-x.
[19] S. Chen, Y. Gao, F. Chen, T.B. Wang, ANLN serves as an oncogene in bladder urothelial carcinoma via activating JNK signaling pathway, Urol. Int. 107 (2023) 310–320, https://doi.org/10.1159/000524204.
[20] T.W. Li, J.X. Fu, Z.X. Zeng, D. Cohen, J. Li, Q.M. Chen, B. Li, X.S. Liu, TIMER2.0 for analysis of tumor-infiltrating immune cells, Nucleic Acids Res. 48 (2020) W509–W514, https://doi.org/10.1093/nar/gkaa407.
[21] M.I. Love, W. Huber, S. Anders, Moderated estimation of fold change and dispersion for RNA-seq data with DESeq2, Genome Biol. 15 (2014). ARTN 55010.1186/s13059-014-0550-8.
[22] Z.F. Tang, C.W. Li, B.X. Kang, G. Gao, C. Li, Z.M. Zhang, GEPIA: a web server for cancer and normal gene expression profiling and interactive analyses, Nucleic Acids Res. 45 (2017) W98–W102, https://doi.org/10.1093/nar/gkx247.
[23] S.E. McGeary, K.S. Lin, C.Y. Shi, T.M. Pham, N. Bisaria, G.M. Kelley, D.P. Bartel, The biochemical basis of microRNA targeting efficacy, Science 366 (2019) 1470. ARTN eaav174110.1126/science.aav1741.
[24] J.H. Li, S. Liu, H. Zhou, L.H. Qu, J.H. Yang, starBase v2.0: decoding miRNA-ceRNA, miRNA-ncRNA and protein-RNA interaction networks from large-scale CLIP-Seq data, Nucleic Acids Res. 42 (2014) D92–D97, https://doi.org/10.1093/nar/gkt1248.
[25] K.R. Zhou, S. L, L. Cai, et al., ENCORI: the encyclopedia of RNA interactomes. https://starbase.sysu.edu.cn/index.php. (Accessed 15 July 2023).
[26] Y.H. Chen, X.W. Wang, miRDB: an online database for prediction of functional microRNA targets, Nucleic Acids Res. 48 (2020) D127–D131, https://doi.org/10.1093/nar/gkz757.
[27] Y. Yi, Y. Zhao, C.H. Li, L. Zhang, H.Y. Huang, Y.N. Li, L.L. Liu, P. Hou, T.Y. Cui, P. W. Tan, et al., RAID v2.0: an updated resource of RNA-associated interactions across organisms, Nucleic Acids Res. 45 (2017) D115–D118, https://doi.org/10.1093/nar/gkw1052.
[28] D. Szklarczyk, R. Kirsch, M. Koutrouli, K. Nastou, F. Mehryary, R. Hachilif, A. L. Gable, T. Fang, N.T. Doncheva, S. Pyysalo, et al., The STRING database in 2023: protein-protein association networks and functional enrichment analyses for any sequenced genome of interest, Nucleic Acids Res. (2022), https://doi.org/10.1093/nar/gkac1000.
[29] B.T. Sherman, M. Hao, J. Qiu, X.L. Jiao, M.W. Baseler, H.C. Lane, T. Imamichi, W. Z. Chang, DAVID: a web server for functional enrichment analysis and functional annotation of gene lists (2021 update), Nucleic Acids Res. 50 (2022) W216–W221, https://doi.org/10.1093/nar/gkac194.
[30] K.J. Livak, T.D. Schmittgen, Analysis of relative gene expression data using real-time quantitative PCR and the 2(T)(-Delta Delta C) method, Methods 25 (2001) 402–408, https://doi.org/10.1006/meth.2001.1262.
[31] B. Chen, M. K, C.L. Liu, A.M. Newman, A.A. Alizadeh, Profiling tumor infiltrating immune cells with CIBERSORT, Methods Mol. Biol. (2018) 243–259, https://doi.org/10.1007/978-1-4939-7493-1_12.
[32] S. Hänzelmann, R. Castelo, J. Guinney, GSVA: gene set variation analysis for microarray and RNA-Seq data, BMC Bioinf. 14 (2013), https://doi.org/10.1186/1471-2105-14-7. Artn 7.
[33] A. Mayakonda, D.C. Lin, Y. Assenov, C. Plass, H.P. Koeffler, Maftools: efficient and comprehensive analysis of somatic variants in cancer, Genome Res. 28 (2018) 1747–1756, https://doi.org/10.1101/gr.239244.118.
[34] D. Maeser, R.F. Gruener, R.S. Huang, oncoPredict: an R package for predicting in vivo or cancer patient drug response and biomarkers from cell line screening data, Brief Bioinform (2021) 22. ARTN bbab26010.1093/bib/bbab260.
[35] IARC. Latest global cancer data: cancer burden rises to 19.3 million new cases and 10.0 million cancer deaths in 2020. Retrieved December 16, 2020, from https://www.iarc.fr/fr/news-events/latest-global-cancer-data-cancer-burden-rises-to-19-3-million-new-cases-and-10-0-million-cancer-deaths-in-2020/.Availableonline: (accessed on.
[36] H. Rastad, P. Samimisedeh, M.S. Alan, E.J. Afshar, J. Ghalami, M. Hashemnejad, M.S. Alan, The role of lncRNA CERS6-AS1 in cancer and its molecular mechanisms: a systematic review and meta-analysis, Pathol. Res. Pract. (2023) 241. ARTN 15424510.1016/j.prp.2022.154245.
[37] F. Teng, J.X. Zhang, Q.M. Chang, X.B. Wu, W.G. Tang, J.F. Wang, J.F. Feng, Z. P. Zhang, Z.Q. Hu, LncRNA MYLK-AS1 facilitates tumor progression and angiogenesis by targeting miR-424-5p/E2F7 axis and activating VEGFR-2 signaling pathway in hepatocellular carcinoma, J Exp Clin Canc Res 39 (2020). ARTN 23510.1186/s13046-020-01739-z.
[38] N. Dastmalchi, M.A. Hosseinpourfeizi, S.M.B. Khojasteh, B. Baradaran, R. Safaralizadeh, Tumor suppressive activity of miR-424-5p in breast cancer cells through targeting PD-L1 and modulating PTEN/PI3K/AKT/mTOR signaling pathway, Life Sci. 259 (2020). ARTN 11823910.1016/j.lfs.2020.118239.
[39] N.M. Tuan, C.H. Lee, Role of anillin in tumour: from a prognostic biomarker to a novel target, Cancers 12 (2020). ARTN 160010.3390/cancers12061600.
[40] K. Oegema, M.S. Savoian, T.J. Mitchison, C.M. Field, Functional analysis of a human homologue of the actin binding protein anillin suggests a role in cytokinesis, J. Cell Biol. 150 (2000) 539–551, https://doi.org/10.1083/jcb.150.3.539.
[41] J. Yao, R.Y. Gao, M.H. Luo, D.F. Li, L.L.Z. Guo, Z.C. Yu, F. Xiong, C. Wei, B.H. Wu, Z.L. Xu, et al., Exosomal LINC00460/miR-503-5p/ANLN positive feedback loop aggravates pancreatic cancer progression through regulating T cell-mediated cytotoxicity and PD-1 checkpoint, Cancer Cell Int. (2022) 22. ARTN 39010.1186/s12935-022-02741-5.
[42] C. Yang, L. Liu, C. Gao, G. Zhang, Y.S. Zhang, S. Zhang, J.P. Li, Y.J. Liu, Circ_0,007,331 promotes the PTX resistance and progression of breast cancer via miR-200b-3p/ANLN, J. Surg. Res. 279 (2022) 619–632, https://doi.org/10.1016/j.jss.2022.05.004.
[43] X.L. Wu, Y. Ren, R. Yao, L.L. Zhou, R.H. Fan, Circular RNA circ-MMP11 contributes to lapatinib resistance of breast cancer cells by regulating the miR-153-3p/ANLN Axis, Front. Oncol. (2021) 11. ARTN 63996110.3389/fonc.2021.639961.
[44] K.J. Liu, L. Cui, C.Q. Li, C.F. Tang, Y.M. Niu, J. Hao, Y. Bu, B.D. Chen, Pan-cancer analysis of the prognostic and immunological role of ANLN: an onco-immunological biomarker, Front. Genet. 13 (2022). ARTN 92247210.3389/fgene.2022.922472.
[45] Y. Xiao, D.H. Yu, Tumor microenvironment as a therapeutic target in cancer, Pharmacol. Therapeut. (2021) 221. ARTN 10775310.1016/j.pharmthera.2020.107753.
[46] L. Long, C. Zhao, M. Ozarina, X.D. Zhao, J. Yang, H.L. Chen, Targeting immune checkpoints in lung cancer: current landscape and future prospects, Clin. Drug Invest. 39 (2019) 341–353, https://doi.org/10.1007/s40261-018-00746-5.
[47] S.S. Hwang, J. Lim, Z.B. Yu, P. Kong, E. Sefik, H. Xu, C.C.D. Harman, L.K. Kim, G. R. Lee, H.B. Li, et al., mRNA destabilization by BTG1 and BTG2 maintains T cell quiescence, Science 367 (2020) 1255, https://doi.org/10.1126/science.aax0194.
[48] R.E. Tay, E.K. Richardson, H.C. Toh, Revisiting the role of CD4(+)T cells in cancer immunotherapy-new insights into old paradigms, Cancer Gene Ther. 28 (2021) 5–17, https://doi.org/10.1038/s41417-020-0183-x.
[49] L.M. Williams, G. Ricchetti, U. Sarma, T. Smallie, B.M.J. Foxwell, Interleukin-10 suppression of myeloid cell activation - a continuing puzzle, Immunology 113 (2004) 281–292, https://doi.org/10.1111/j.1365-2567.2004.01988.x.
[50] M.C. Duan, X.N. Zhong, G.N. Liu, J.R. Wei, The Treg/Th17 paradigm in lung cancer, J Immunol Res. 2014 (2014), https://doi.org/10.1155/2014/730380, 730380 Epub 2014 Apr 29. PMID: 24872958; PMCID: PMC4020459.
[51] J.H. Liu, Z.C. Chen, Y.Q. Li, W.J. Zhao, J.B. Wu, Z. Zhang, PD-1/PD-L1 checkpoint inhibitors in tumor immunotherapy, Front. Pharmacol. 12 (2021). ARTN 73179810.3389/fphar.2021.731798.
[52] Y. Latchman, C. Wood, T. Chemova, Y. Iwai, N. Malenkovich, A. Long, K. Bourque, V. Boussiotis, H. Nishimura, T. Honjo, et al., PD-L2, a novel B7 homologue, is a second ligand for PD-1 and inhibits T cell activation, Faseb. J. 15 (2001) A345.
[53] E. Ruffo, R.C. Wu, T.C. Bruno, C.J. Workman, D.A.A. Vignali, Lymphocyte-activation gene 3 (LAG3): the next immune checkpoint receptor, Semin. Immunol. 42 (2019). ARTN 10130510.1016/j.smim.2019.101305.
[54] J.J. Havel, D. Chowell, T.A. Chan, The evolving landscape of biomarkers for checkpoint inhibitor immunotherapy, Nat. Rev. Cancer 19 (2019) 133–150, https://doi.org/10.1038/s41568-019-0116-x.
[55] O. Hassin, M. Oren, Drugging p53 in cancer: one protein, many targets, Nat. Rev. Drug Discov. 22 (2023) 127–144, https://doi.org/10.1038/s41573-022-00571-8.